Preparation and performance of dye-sensitized solar cells based on ZnO-modified TiO$_2$ electrodes

Sheng-jun Li[1,2], *Yuan Lin*[2], *Wei-wei Tan*[2], *Jing-bo Zhang*[2], *Xiao-wen Zhou*[2], *Jin-mao Chen*[2], *and Zeng Chen*[1]

1) College of Physics and Electrics, He'nan University, Kaifeng 475004, China

2) Beijing National Laboratory for Molecular Sciences, Key Laboratory of Photochemistry, Institute of Chemistry, Chinese Academy of Sciences, Beijing 100080, China

Abstract: The ZnO-modified TiO$_2$ electrode was prepared by adding Zn(CH$_3$COO)$_2$·2H$_2$O to the TiO$_2$ colloid during the sol-gel production process, and was used in dye-sensitized solar cells (DSCs). The open circuit voltage (V_{OC}) and fill factor (ff) of the cells were improved significantly. The performances of the ZnO-modified TiO$_2$ electrode such as dark current, transient photocurrent, impedance, absorption spectra, and flat band potential (V_{fb}) were investigated. It is found that the interface charge recombination impedance increases and V_{fb} shifts about 200 mV toward the cathodic potential. The effect mechanism of ZnO modification on the performance of DSCs may be that ZnO occupies the surface states of the TiO$_2$ film.

Keywords: dye-sensitized solar cells; TiO$_2$ electrode; modification; photoelectrochemical properties

1. Introduction

Dye-sensitized solar cells (DSCs) based on TiO$_2$ nanocrystalline electrodes have attracted the attention of scientists because of their high performance and low-cost production [1-5]. Although DSCs based on other nanocrystalline semiconductors such as ZnO and SnO$_2$ are also prepared, most of them do not have the conversion efficiency as high as the efficiency of TiO$_2$ cells [6-8]. The major parameters of DSCs are the short circuit current density (J_{SC}), open circuit voltage (V_{OC}), and fill factor (ff) of the photocurrent-voltage (I-V) curves. The charge recombination at the TiO$_2$/dye/electrolyte interface has a serious effect on J_{SC}, V_{OC}, and ff of the solar cells [9-10]. To reduce the recombination reactions, several research groups modify TiO$_2$ with metal oxides such as Nb$_2$O$_5$, MgO, ZnO, and so on [11-15].

Kim *et al*. [15] obtained ZnO-modified TiO$_2$ by spraying the ethanol solution of TiO$_2$ powder and ZnCl$_2$ into liquid N$_2$, and used the nanocrystalline electrode in the flexible dye-sensitized solar cells. The conversion efficiency (η) increased from 0.71% to 1.21%. Kim *et al*. [16] prepared ZnO-coated TiO$_2$ by the thermal chemical vapor deposition method. The J_{SC} and V_{OC} of the cells were improved by 12% and 17%, respectively. Roh *et al.* [17] improved the conversion efficiency by the chemically deposited ZnO layer on TiO$_2$ electrodes.

In this paper, ZnO modified TiO$_2$ electrodes were prepared by adding Zn(CH$_3$COO)$_2$·2H$_2$O to the TiO$_2$ colloid during the sol-gel production process. Some experiments, such as dark current, transient photocurrent, impedance, absorption spectra, and flat band potential, were carried out to explore the causes for the enhancement of the photoelectrochemical properties of DSCs.

Ⓐ Springer

2. Experimental

2.1. Preparation of ZnO-modified TiO₂ electrodes

TiO$_2$ colloids were prepared by hydrolyzing the mixture of titanium (IV) isopropoxide (Aldrich) and isopropyl alcohol in the presence of distilled acetic acid (pH=2) followed by autoclaving at 250ºC for 12 h. After the hydrothermal treatment, different contents of Zn(CH$_3$COO)$_2$·2H$_2$O were added to the TiO$_2$ colloidal solution. The colloidal solution was condensed in a rotary evaporator. The Zn/Ti molar ratio was controlled to be 0.01, 0.025, 0.5, and 0.1, respectively. After the concentration, the TiO$_2$ colloidal paste was doctor-bladed onto the clean transparent conduction glass sheets (FTO, 30 Ω·square^{-1}, F-doped SnO$_2$). To control the thickness of the film, two edges of the transparent conduction glass substrate were covered with adhesive tapes. After drying in air, the samples were heated for 30 min at 450ºC, resulting in anatase TiO$_2$ nanoparticle film electrodes. The prepared nanocrystalline TiO$_2$ films were conserved in a desiccator.

2.2. Characterization of the TiO₂ film

The crystalline phases of the samples were characterized by a Rigaku D/max2500 X-ray powder diffractometer (XRD) with a monochromatized Cu K$_\alpha$ irradiation. The morphologies of the samples were determined using a Hitachi S-4300F field emission scanning electron microscope (SEM).

2.3. Solar cell fabrication

Nanoporous TiO$_2$ films were dipped into the 5×10^{-4} mol ethanol solution of *cis*-bis(thiocyanato)-*N,N'*-bis(2,2'-bipyridyl-4,4'-dicarboxylate) ruthenium (II) for about 12 h. The counter electrode was Pt foil. The mixture of ethylene carbonate (EC, Acros) and propylene carbonate (PC, Acros) (EC:PC=5:5, *V/V*) containing 0.5 mol KI and 0.05 mol I$_2$ expressed as EC/PC/KI/I$_2$ was selected to be the electrolyte of DSCs. The counter electrode and the dye-sensitized TiO$_2$ electrode were clamped firmly together. The redox electrolyte solution was introduced into the porous nanocrystalline TiO$_2$ film by capillary action [18].

2.4. Photoelectrochemical and electrochemical measurements

The photoelectrochemical characteristics of DSCs were measured by the photocurrent-voltage curve (*I-V* curves) measurement with a potentiostat (EG&G Princeton Applied Research, Model 273) under the simulated solar light. A 250-W tungsten halogen lamp was used as the light source. The incident light intensity was 100 mW·cm^{-2} measured by

350 linear/log optometer (UDT instruments) and the active cell area was 0.2 cm^2. The dark current and transient photocurrent pattern of DSCs were measured using the same potentiostat as the *I-V* curves.

The electrochemical impedance spectra (EIS) and the flat band potential measurement were carried out with a potentiostat (Solartron SI1287) and a frequency response analyzer (Solartron 1255B). The impedance measurement of DSCs was recorded over a frequency range of 0.01-1 MHz with the AC amplitude of 10 mV. The measurement was performed at the open circuit voltage under the same light intensity as the *I-V* curve measurement. The flat band potential was measured by the Mott-Schottky analysis method with the potential range from 0 to −1.0 V [19-20].

3. Results and discussion

Fig. 1 illustrates the XRD patterns of the bare TiO$_2$ and 5at% ZnO-modified TiO$_2$ thin films. The bare TiO$_2$ and 5at% ZnO-modified TiO$_2$ thin films both consist of anatase titania crystals. The diffraction peaks of the 5at% ZnO-modified TiO$_2$ thin film are almost the same as the pure TiO$_2$ film except for a little decrease in the peak intensity. There are no diffraction peaks of ZnO structure, which means that the addition of a small amount of ZnO does not change the structure of anatase-TiO$_2$.
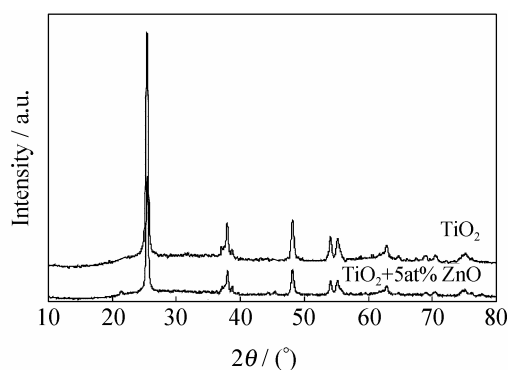

Fig. 1.   XRD patterns of bare TiO₂ and 5at% ZnO-modified TiO₂ thin films.

Fig. 2 shows the SEM micrographs of pure TiO$_2$ and 5at% ZnO-modified TiO$_2$ thin films. After the modification of 5at% ZnO, the morphology of the TiO$_2$ thin film has no significant change.

The electron dispersive X-ray (EDX) spectrum of the ZnO-modified TiO$_2$ film is shown in Fig. 3. The Zn element is found in the sample, but the quantity of Zn is small which is consistent with the conclusion of the XRD patterns (Fig. 1) and the SEM micrographs (Fig. 2).
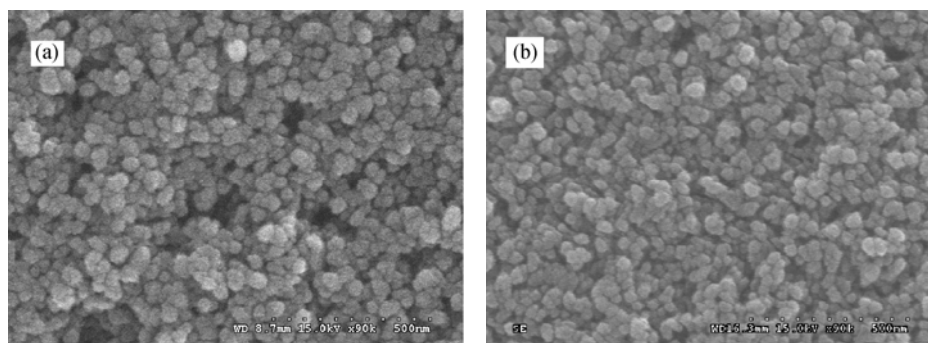
Fig. 2.   SEM micrographs of bare TiO_2 (a) and 5at% ZnO-modified TiO_2 thin films (b).
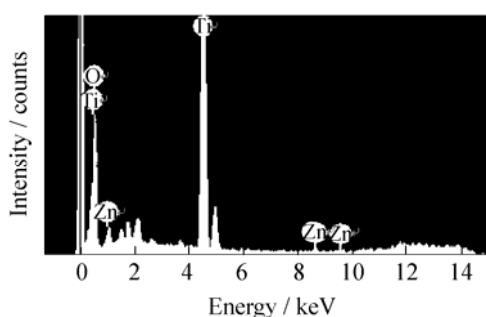

Fig. 3.   EDX spectrum of the 5at% ZnO-modified TiO_2 thin films.

The photoelectric data of the dye-sensitized solar cells using ZnO-modified TiO_2 nanoporous electrodes are summarized in Table 1. The open circuit voltage and fill factor keep increasing with the increase of the Zn content. However, the short circuit current decreases with the increase in Zn/Ti (at%). The conversion efficiency can be enhanced about 0.4% when the Zn content is 5at%. The short circuit current decreases sharply when the Zn content is higher than 5at%, and the conversion efficiency begins to decline.

Table 1.   Photoelectrochemical parameters of DSCs using ZnO-modified TiO_2 nanoporous electrodes

Zn:Ti / at%	J_{SC} / (mA·cm^{-2})	V_{OC} / mV	ff	η / %
0.000	17.0	539	0.55	4.98
0.010	16.2	559	0.56	5.08
0.025	15.7	572	0.59	5.28
0.050	13.0	641	0.65	5.39
0.100	9.3	664	0.67	4.11

The restriction of charge recombination at the TiO_2/dye/electrolyte interface is one important factor for the improvement of V_{OC} and ff of DSCs [9, 12]. The dark current arises from the reduction of triiodide and oxidized dye molecule by conduction band electrons of TiO_2 films. The dark current measurement is an apparent analysis on the interface charge recombination. Fig. 4 addresses the dark cur-

rent for the dye-sensitized solar cells using pure TiO_2 and ZnO-modified TiO_2 nanoporous electrodes. The dark current is significantly reduced by the modification of ZnO. This observation of the reduction of charge recombination is consistent with the reports of Kim *et al.* [16].
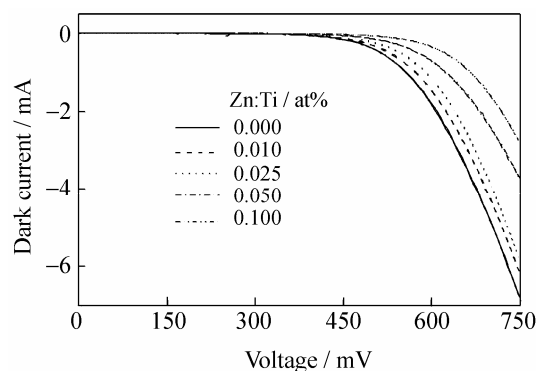

Fig. 4.   Dark current characteristics of DSCs using pure TiO_2 and ZnO-modified TiO_2 nanoporous electrodes.

Fig. 5 shows the electrochemical impedance spectra (EIS) of pure TiO_2 and 5at% ZnO-modified TiO_2 electrodes, where the ReZ and ImZ correspond to the real and imaginary part of the electrochemical impedance, respectively. The illumination condition of the impedance measurement was the same as that of the *I-V* measurement. Three arcs appear in the impedance spectra of the dye-sensitized solar cell using pure TiO_2 which are expressed as their characteristic frequencies ω_1, ω_2 and ω_3. The arcs appear around 2000, 100, and 0.5 Hz, respectively. The three semicircles are separately attributed to the redox reaction at the platinum counter electrode (ω_1), the electron transfer at the TiO_2/dye/electrolyte interface (ω_2), and ion transport within the electrolyte (ω_3) [21-22]. However, only one arc is observed in the impedance spectra of the dye-sensitized solar cell using the 5at% ZnO-modified TiO_2 electrode. This arc appears around 50 Hz which should be caused by the recombination reactions at the TiO_2/dye/electrolyte interface

(ω_2). The other two arcs (ω_1 and ω_3) may be hidden by the large arc (ω_2). It is noticeable that the recombination reaction impedance (ω_2) has been increased by the modification of 5at% ZnO. It can also be found that the characteristic frequency of (ω_2) of the DSCs using the 5at% ZnO-modified TiO₂ electrode becomes smaller than that of the DSCs using the pure TiO₂ electrode. The inverse of the characteristic frequency of ω_2 has been expressed to be the recombination lifetime of the electron in the conduction band of TiO₂ [23-24]. Therefore, the decrease in the charac-

teristic frequency of ω_2 means that the injected electrons in the TiO₂ conduction band can stay steadily for a longer time in the ZnO-modified TiO₂ electrode. Both the larger impedance and the smaller characteristic frequency of the arc ω_2 should be favorable for the high performance of DSCs. It can be seen that ZnO modification can passivate the surface of the TiO₂ film. The normalized transient photocurrent pattern and absorption spectra of bare TiO₂ and ZnO-modified TiO₂ films were carried out to explore the causes for the changes of photoelectric and impedance performance.
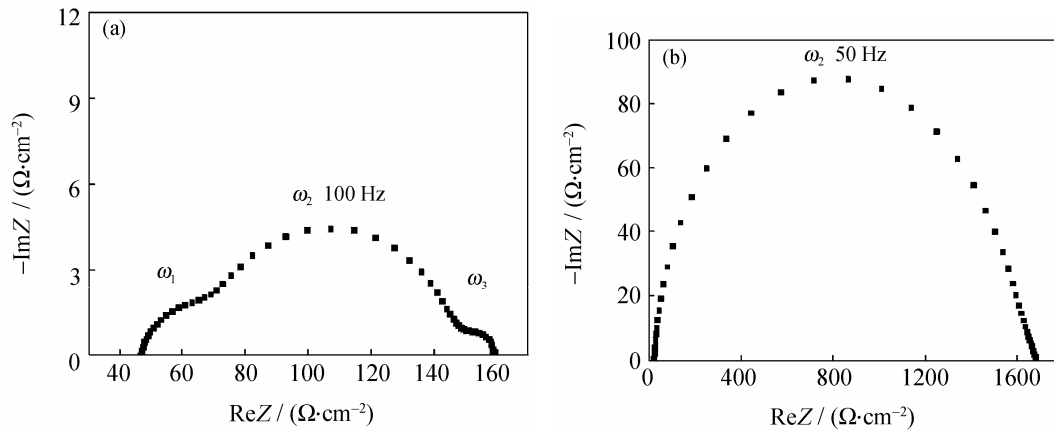

Fig. 5. EIS of DSCs using the bare TiO₂ (a) and 5at% ZnO-modified TiO₂ thin films (b).

Fig. 6 shows the normalized transient photocurrent patterns of DSCs using pure TiO₂ and ZnO-modified TiO₂ nanoporous electrodes. The photocurrent response of the ZnO-modified TiO₂ electrode becomes more rapid than the pure TiO₂ electrode. When the light is switched off, the photocurrent of the ZnO-modified TiO₂ electrode falls faster than the pure TiO₂ electrode. The cause may be that ZnO occupies the surface states of the TiO₂ electrode. The bondage of the electron in the TiO₂ conduction band is reduced and the recombination reaction between the electron and triiodide ion (or oxidized dye molecular) is decreased.
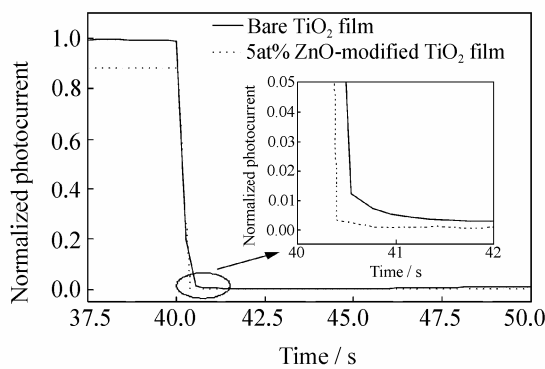
ZnO-modified TiO₂ films. After ZnO modification, the absorption band edge of TiO₂ is blue-shifted which means that the band gap energy of the ZnO-modified TiO₂ film is improved. However, the band gap energy of ZnO is 3.2 eV which is almost the same as that of anatase TiO₂ [25]. The change of the absorption band edge can be that ZnO occupies the surface states of TiO₂ film.
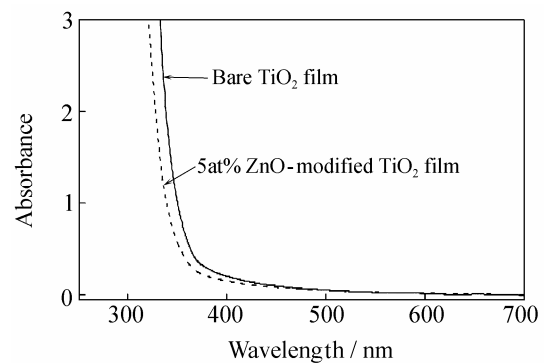

Fig. 7. Absorption spectra of bare TiO₂ and 5at% ZnO-modified TiO₂ thin films.

Fig. 8 shows the Mott-Schottky curves of pure TiO₂ and ZnO-modified TiO₂ films, where C is the space-charge capacitance, V_{fb} is the flat band potential. The plot of C^{-2} *vs.* polarization potential shows an X-intercept corresponding to V_{fb}. The V_{fb} shifts about 200 mV toward the cathodic poten-

Fig. 6. Normalized transient photocurrent patterns of DSCs using the bare TiO₂ and 5at% ZnO-modified TiO₂ thin films.

Fig. 7 shows the absorption spectra of bare TiO₂ and

tial after the ZnO modification of the TiO_2 film which is also one important cause for the improvement of V_{OC} of the DSCs [26]. However, when V_{fb} shifts negatively, the driving force decreases for the charge transfer from the excited dye molecular to the conduction band, resulting in the decline of the photocurrent of DSCs.
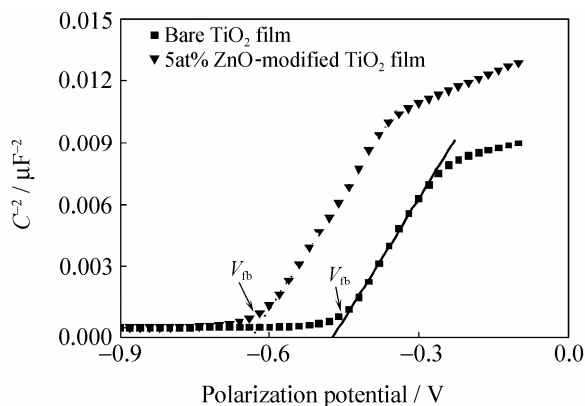
Fig. 8.   Mott-Schottky plots of bare TiO_2 and 5at% ZnO-modified TiO_2 thin films.

To avoid the decline of the photocurrent, V_{fb} of the TiO_2 film should be shifted positively. Li^+ is a strong electroposi-tive cation. After the addition of LiI in the electrolyte, Li^+ will be absorbed on the surface of the TiO_2 electrode and its radius is so small that Li^+ will penetrate into TiO_2 lattice [27-28]. As a result, the energy level of the conduction band of the TiO_2 electrode is enhanced. In this experiment, 0.05 mol LiI was added into the $EC/PC/KI/I_2$ electrolyte.

Fig. 9 and Table 2 show the photoelectric performance of the pure TiO_2 and ZnO-modified TiO_2 electrodes using the electrolyte (EC:PC=1:1, *V/V*)+0.5 mol/L KI+0.05 mol/L I_2+ 0.05 mol/L LiI.
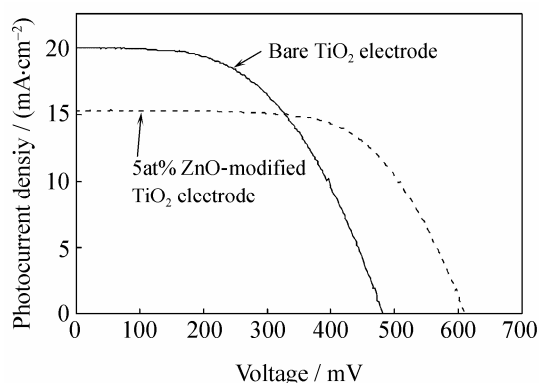
Fig. 9.   Photocurrent-voltage curves of DSCs using the bare TiO_2 and 5at% ZnO-modified TiO_2 electrodes in the $EC/PC/KI/I_2$ electrolyte with 0.05 mol LiI.

The photocurrent is increased significantly for all the DSCs after the addition of LiI. For the pure TiO_2 electrode, the V_{OC} and ff are decreased seriously, and the conversion efficiency has almost no change after the addition of LiI in the electrolyte. However, for the ZnO-modified TiO_2 elec-trodes, the conversion efficiency is improved from 5.39% to 5.89%.

Table 2.   Photoelectrochemical parameters of DSCs using the ZnO-modified TiO_2 nanoporous electrode in the $EC/PC/KI/I_2$ electrolyte with 0.05 mol LiI

Zn:Ti / at%	J_{SC} / (mA·cm^{-2})	V_{OC} / mV	ff	η / %
0.00	20.0	484	0.52	4.97
0.05	15.3	611	0.63	5.89

4. Conclusion

The ZnO-modified TiO_2 electrode was prepared by add-ing $Zn(CH_3COO)_2·2H_2O$ to the TiO_2 colloid during the sol-gel production process. The crystalline phases and mor-phologies of TiO_2 electrodes have almost no change after ZnO modification. However, the V_{OC} and ff of DSCs are improved significantly. The conversion efficiency can be enhanced from 4.98% to 5.39% when the Zn content is 5at%. After ZnO modification, the dark current of DSCs de-clines and the interface charge recombination impedance increases significantly. On the other hand, V_{fb} shifts about 200 mV toward the cathodic potential which is also one important cause for the improvement of V_{OC}. The effect mechanism of ZnO modification on the performance of DSCs may be that ZnO occupies the surface states of the TiO_2 film. In the electrolyte (EC:PC=1:1, *V/V*)+0.5 mol/L KI+0.05 mol/L I_2+0.05 mol/L LiI, the conversion efficiency of the cell using ZnO-modified TiO_2 is 5.89%, which is im-proved by about 20%.

References

[1]   B. O'Regan and M. Grätzel, A low-cost, high-efficiency solar cell based on dye-sensitized colloidal TiO_2 film, *Nature*, 353(1991), p.737.

[2]   C.J. Barbé, F. Arendse, P. Comte, *et al*., Nanocrystalline tita-nium oxide electrodes for photovoltaic applications, *J. Am. Ceram. Soc.*, 80(1997), p.3157.

[3]   M. Grätzel, Photoelectrochemical cells, *Nature*, 414(2001), p.338.

[4]   J. Yamamoto, A. Tan, R. Shiratsuchi, *et al*., A 4% efficient dye-sensitized solar cell fabricated from cathodically electro-synthesized composite titania films, *Adv. Mater.*, 15(2003), p.1823.

[5]   W. Kubo, T. Kitamura, K. Hanabusa, *et al*., Quasi-solid-state dye-sensitized solar cells using room temperature molten salts and a low molecular weight gelator, *Chem. Commun.*, (2002), p.374.

[6] K. Tennakone, G.R.R.A. Kumara, I.R.M. Kottegoda, *et al.*, An efficient dye-sensitized photoelectrochemical solar cell made from oxides of tin and zinc, *Chem. Commun.*, 1999, No.1, p.15.

[7] X. Sheng, Y. Zhao, J. Zhai, *et al.*, Electro-hydrodynamic fabrication of ZnO-based dye sensitized solar cells, *Appl. Phys. A*, 87(2007), p.715.

[8] N.G. Park, M.G. Kang, K.M. Kim, *et al.*, Morphological and photoelectrochemical characterization of core-shell nanoparticle films for dye-sensitized solar cells: ZnO type shell on SnO$_2$ and TiO$_2$ cores, *Langmuir*, 20(2004), p.4246.

[9] E. Palomares, J.N. Clifford, S.A. Haque, *et al.*, Control of charge recombination dynamics in dye sensitized solar cells by the use of conformally deposited metal oxide blocking layers, *J. Am. Chem. Soc.*, 125(2003), p.475.

[10] J. Van de Lagemaat, N.G. Park, and A.J. Frank, Influence of electrical potential distribution charge transport and recombination on the photopotential and photocurrent conversion efficiency of dye-sensitized nanocrystalline TiO$_2$ solar cells: A study by electrical impedance and optical modulation techniques, *J. Phys. Chem. B*, 104(2000), p.2044.

[11] S.G. Chen, S. Chappel, Y. Diamant, *et al.*, Preparation of Nb$_2$O$_5$ coated TiO$_2$ nanoporous electrodes and their application in dye-sensitized solar cells, *Chem. Mater.*, 13(2001), p.4629.

[12] H.S. Jung, J.K. Lee, and M. Nastasi, Preparation of nanoporous MgO-coated TiO$_2$ nanoparticles and their application to the electrode of dye-sensitized solar cells, *Langmuir*, 21(2005), p.10332.

[13] X.T. Zhang, I. Sutanto, T. Taguchi, *et al.*, Al$_2$O$_3$-coated nanoporous TiO$_2$ electrode for solid-state dye-sensitized solar cell, *Sol. Energy. Mater. Sol. Cells*, 80(2003), p.315.

[14] Z.S. Wang, M. Yanagida, K. Sayama, *et al.*, Electronic-insulating coating of CaCO$_3$ on TiO$_2$ electrode in dye-sensitized solar cells: Improvement of electron lifetime and efficiency, *Chem. Mater.*, 18(2006), p.2912.

[15] S.S. Kim, J.H. Yum, and Y.E. Sung, Flexible dye-sensitized solar cells using ZnO coated TiO$_2$ nanoparticles, *J. Photochem. Photobiol. A*, 171(2005), p.269.

[16] K.E. Kim, S.R. Jang, J. Park, *et al.*, Enhancement in the performance of dye-sensitized solar cells containing ZnO-covered TiO$_2$ electrodes prepared by thermal chemical vapor deposition, *Sol. Energy. Mater. Sol. Cells*, 91(2007), p.366.

[17] S.J. Roh, R.S. Mane, S.K. Min, *et al.*, Achievement of 4.51% conversion efficiency using ZnO recombination barrier layer in TiO$_2$ based dye-sensitized solar cells, *Appl. Phys. Lett.*, 89(2006), Art. No.253512.

[18] M.K. Nazeeruddin, A. Kay, I. Rodicio, *et al.*, Conversion of light to electricity by *cis*-X$_2$bis(2,2'-bipyridyl-4,4'-dicarboxylate) ruthenium(II) charge transfer sensitizers (X=Cl⁻, Br⁻, I⁻, CN⁻, and SCN⁻) on nanocrystalline TiO$_2$ electrodes, *J. Am. Chem. Soc.*, 115(1993), p.6382.

[19] M. Wang, Q.L. Zhang, Y.X. Weng, *et al.*, Investigation of mechanisms of enhanced open-circuit photovoltage of dye-sensitized solar cells based the electrolyte containing 1-hexyl-3-methylimidazolium iodide, *Chin. Phys. Lett.*, 23(2006), p.724.

[20] G. Redmond and D. Fitzmaurice, Spectroscopic determination of flatband potentials for polycrystalline TiO$_2$ electrodes in nonaqueous solvents, *J. Phys. Chem.*, 97(1993), p.1426.

[21] T. Hoshikawa, R. Kikuchi, and K.J. Eguchi, Impedance analysis for dye-sensitized solar cells with a reference electrode, *Electroanal. Chem.*, 588(2006), p.59.

[22] N. Koide, A. Islam, Y. Chiba, *et al.*, Improvement of efficiency of dye-sensitized solar cells based on analysis of equivalent circuit, *J. Photochem. Photobiol. A*, 182(2006), p.296.

[23] G. Schlichthörl, S.Y. Huang, J. Sprague, *et al.*, Band edge movement and recombination kinetics in dye-sensitized nanocrystalline TiO$_2$ solar cells: A study by intensity modulated photovoltage spectroscopy, *J. Phys. Chem. B*, 101(1997), p.8141.

[24] L. Dloczik, O. Шeperuma, I. Lauermann, *et al.*, Dynamic response of dye-sensitized nanocrystalline solar cells: characterization by intensity-modulated photocurrent spectroscopy, *J. Phys. Chem. B*, 101(1997), p.10281.

[25] A.L. Linsebigler, G. Lu, and J.T. Yates, Photocatalysis on TiO$_2$ surfaces: Principles, mechanisms, and selected results, *Chem. Rev.*, 95(1995), p.735.

[26] X. Yin, H. Zhao, L.P. Chen, *et al.*, The effects of pyridine derivative additives on interface processes at nanocrystalline TiO$_2$ thin film in dye-sensitized solar cells, *Surf. Interface Anal.*, 39(2007), p.809.

[27] Y. Liu, A. Hagfeldt, X.R. Xiao, *et al.*, Investigation of influence of redox species on the interfacial energetics of a dye-sensitized nanoporous TiO$_2$ solar cell, *Sol. Energy. Mater. Sol. Cells*, 55(1998), p.267.

[28] D.F. Watson and G.J. Meyer, Cation effects in nanocrystalline solar cells, *Coord. Chem. Rev.*, 248(2004), p.1391.